

# Using the Angle Index to Assess COVID-19 Damage at the Early Stage and Throughout 2020 in Comparison of Mathematical Models

**Daw-Hsin Yang**

Chi Mei Foundation Hospital: Chi Mei Medical Center

**Tsair-wei Chien**

Chi Mei Medical Center <https://orcid.org/0000-0003-1329-0679>

**Willy Chou**

Chi Mei Medical Center

**Kang-Ting Tsai** (✉ [irised57@yahoo.com.tw](mailto:irised57@yahoo.com.tw))

Center for Integrative Medicine, ChiMei Medical Center

---

## Research

**Keywords:** item response theory, ogive curve, IRT model, exponential growth model, quadratic equation model, MAPE, R-square, COVID-19

**Posted Date:** June 30th, 2021

**DOI:** <https://doi.org/10.21203/rs.3.rs-643679/v1>

**License:**   This work is licensed under a Creative Commons Attribution 4.0 International License.

[Read Full License](#)

---

# Using the Angle Index to Assess COVID-19 Damage at the Early Stage and Throughout 2020 in Comparison of Mathematical Models

Daw-Hsin Yang, MD <sup>1</sup>, Tsair-Wei Chien<sup>2</sup>, MBA<sup>2</sup>, Willy Chou, MD <sup>3,4\*</sup>, Kang-Ting Tsai, MD <sup>5,6,7\*</sup>

<sup>1</sup> Department of Gastrointestinal Hepatobiliary, Chiali Chi-Mei Hospital, Tainan, Taiwan

<sup>2</sup> Department of Medical Research, Chi-Mei Medical Center, Tainan, Taiwan

<sup>3</sup> Department of physical medicine and rehabilitation, Chiali Chi-Mei Hospital, Tainan, Taiwan

<sup>4</sup> Department of Physical Medicine and Rehabilitation, Chung San Medical University Hospital, Taichung 400, Taiwan.

<sup>5</sup> Center for Integrative Medicine, ChiMei Medical Center, 700 Tainan, Taiwan

<sup>6</sup> Department of Geriatrics and Gerontology, Chi Mei Medical Center, 700 Tainan, Taiwan

<sup>7</sup> Department of Senior Welfare and Services, Southern Taiwan University of Science and Technology, 700 Tainan, Taiwan

Running title: Mathematical model of COVID-19 in comparison

Word count: 2,835, Table:0, Figure: 7

**\*Corresponding Author**

Kang-Ting Tsai

Chi-Mei Medical Center, 901 Chung Hwa Road, Yung Kung Dist., Tainan 710, Taiwan

E-mail: irised57@yahoo.com.tw

Daw-Hsin Yang (DH): dawhsin@yahoo.com.tw

Tsair-Wei Chien(TW): rasch.smile@gmail.com

Willy Chou(WC): ufan0101@ms22.hinet.net

Kang-Ting Tsai (KT): irised57@yahoo.com.tw

## Abstract

**Background:** The negative impacts of COVID-19 are commonly assessed using the cumulative numbers of confirmed cases. However, whether different mathematical models yield disparate results based on varying time frames remains unclear. The angle index was proposed in this study to measure the negative impacts of the COVID-19 pandemic.

**Methods:** Data used in this work were downloaded from the GitHub website. Three mathematical models were examined in two time-frame scenarios during the COVID-19 pandemic (early 20-day stage and the entire year of 2020). The angle index was determined by the ratio of a cumulative number of confirmed cases (CNCCs) divided by the inflection point. To evaluate the model's accuracy and the prediction power in the two time-frame scenarios, both the  $R^2$  model and mean absolute percentage error (MAPE) were used. The following findings were obtained: (1) the exponential growth (EXPO) and item response theory (IRT) models are superior to the quadratic equation (QE) model at the earlier outbreak stage; (2) the IRT model had a higher model  $R^2$  and smaller MAPE than the EXPO model in 2020; (3) Hubei Province in China had the highest angle index at the early stage; and (4) India, California (US), and the UK had the highest angle indexes in 2020.

**Results:** The following findings were obtained: (1) the exponential growth (EXPO) and item response theory (IRT) models are superior to the quadratic equation (QE) model at the earlier outbreak stage; (2) the IRT model had a higher model  $R^2$  and smaller MAPE than the EXPO model in 2020; (3) Hubei Province in China had the highest angle index at the early stage; and (4) India, California (US), and the UK had the highest angle indexes in 2020.

**Conclusion:** The three proposed models are available for measuring the negative impacts of COVID-19. Thus, the IRT model (superior in the long term) and the EXPO model (better at the early stage) are recommended to epidemiologists and policymakers for the effective management of disease outbreak.

**Keywords:** item response theory; ogive curve; IRT model; exponential growth model; quadratic equation model; MAPE; R-square; COVID-19

## **Background:**

In the field of epidemiology, an “outbreak” refers to a sudden increase in occurrences of a disease in a particular time and place. In comparison, a “pandemic” is defined as a near-global disease outbreak in which multiple countries across the world are infected [1]. Using the cumulative numbers of the confirmed case (CNCCs) is a commonly used method in assessing the negative impacts of the COVID-19 outbreak (ImpactCOVID for short) [2–5]. However, its evaluation might be questionable due to the fact that it does not consider the length of infected days effectively under control (known as “LID”). This concept is similar to the inflection

point (IP) days on a given ogive curve, wherein the curvature changes sign from an increasing concave (concave downward) to a decreasing convex (concave upward) shape, or vice versa [1]. For this reason, combining both the CNCC and LID for measuring the negative impacts of the pandemic is reasonable and necessary.

## **1.1. Literature Review**

### **1.1.1. Using the IP and CNCC to Assess the Negative Impacts of COVID-19**

If both CNCCs and LID are considered, the impact (computed as  $CNCCs \div LID$ ) is similar to the journal impact factor (i.e.,  $IF = citations \div publications$ ). Many metrics have been proposed to improve the drawbacks of impact factor, such as the h- and x-indexes [6,7]. On the one hand, the h-index is determined by the maximum square that fits under an author's citation curve when plotting the number of citations in decreasing order; on the other hand, the x-index is determined by the maximum area rectangle that fits under the curve [7]. Then, all excessive citations and publications are excluded from computing the metrics.

To identify the negative impact, past studies proposed the IPcase index, which used the rectangle area ("core area") multiplied by the IP days and the CNCC [1,4]. However, the IPcase index has two drawbacks: (i) it has an identical value but with a distinct meaning (e.g.,  $IPcase\ index = CNCC \times IP = height \times width = 100 = 4 \times 25 = 25 \times 4 = 10 \times 10$ ); (ii) it does not denote the momentum of a sudden ImpactCOVID. Thus, the improved angle index is defined as follows:

$$\text{Angle index} = \theta = \text{Degrees}(\text{Atan}(\frac{\Delta CNCC_k}{\Delta IP_k})), \quad (1)$$

where Degrees() and Atan() are derived from the functions in Microsoft Excel. For instance,  $\Delta IP = 7$  days,  $\Delta CNCC = 27,100 - 11,177 = 15,934$ , ratio =  $15,934/(7-1) = 2653.8$ ,  $\theta = \text{DEGREES}(\text{ATAN}(2653.8)) = 89.97$ . The angle index ranges from 0 to 90, wherein a higher  $\theta$  value means a greater negative impact (“severely hit”) of COVID-19 in a given country or region. The premise determines the IP days (similar to the LID defined in the previous section) before calculating the angle index for a specific country/region.

### 1.1.2. Using Mathematical Models to Determine the IP

Traditionally, the mean number of confirmed cases across varying periods (number of days) yields significantly different IP days, even though the daily number of confirmed cases (computed based on the previous seven days) can be applied to estimate the “observed” IP days [8,9]. In this case, using a mathematical model to determine the “expected” IP days is more objective than referring to the IP days based on the mean number of confirmed cases, which is typically employed in practice [2].

Although many mathematical models [2,10–19] have been proposed to predict the number of COVID-19 cases, none of those models—except one using item response theory (IRT) [2]—have been applied to determine the IP days on a given ogive curve. In relation to this, the differences among mathematical models in terms of model accuracy (MA) and prediction power (PP) should be investigated. Notably, MA and PP can be measured by the  $R^2$  model and

mean absolute percentage error (MAPE), respectively (see the Methods section for details on  $R^2$  and MAPE).

With such information, we are thus motivated to compare the differences in MA and PP in COVID-19 models to obtain a better understanding of their attributes and the meaning of the angle indexes computed for each country/region.

## **1.2. Main Goals**

This study aimed (i) to compare the differences in MA and PP among the three proposed COVID-19 models, (ii) to develop an angle index that can be objectively used to evaluate the ImpactCOVID, and (iii) to compare the differences in angle indexes across countries/regions around the world.

## **Materials**

### **2.1. Data Source**

The COVID-19 data were downloaded from the GitHub website [20] for countries/regions (see Additional file 1). All downloaded data are publicly released on the website [20]. Ethical approval was not necessary for this study since all the data were obtained from the GitHub website.

### **2.2. Introducing the Mathematical Models**

#### **2.2.1. The EXPO Model**

The non-linear regression and iterative methods are commonly used in the study of natural

science [21,22]. The exponential growth (EXPO) has been proposed to construct the COVID-19 prediction model at an early outbreak stage [18] based on the daily growth rate (GR) of confirmed cases using Equation (2):

$$GR_{n-1} = \frac{case_n - case_{n-1}}{case_{n-1}}, \quad (2)$$

$$GR_{t-1} = ae^{-\beta t}, \quad (3)$$

where  $case_n$  and  $case_{n-1}$  are the daily number of confirmed cases on day  $n$  and  $n - 1$ , respectively. The GR can be modeled in Equation (3), where  $a$  is a constant that represents the growth rate at  $t = 0$ ,  $\beta$  is an attenuation coefficient that indicates the efficiency of government isolation and quarantine, and  $t$  is the time representing the evolution of the epidemic [18].

Based on Equation (2), the nonlinear regression and iterative methods can be constructed to predict the CNCC using Equation (4):

$$CNCC_k = CNCC_0 \times \prod_{i=1}^k (1 + ae^{-\beta t}). \quad (4)$$

where  $CNCC_0$  and  $CNCC_k$  are the cumulative number of confirmed cases at  $t = 0$  and the expected CNCC at  $t = k$ , respectively.

### 2.2.2. The IRT Model

The item response model (IRT) was proposed in 2021 [1,4] using Equation (5):

$$P(\theta) = \frac{1}{1 + e^{-1.7*a(\theta-b)}} = \frac{e^{1.7*a(\theta-b)}}{1 + e^{1.7*a(\theta-b)}}, \quad (5)$$

where parameters  $a$  and  $b$  represent the discrimination (i.e., the slope from 0 to 4) and the difficulty (i.e., a location from  $-5$  to  $5$ , where the figure toward the left indicates that the outbreak occurred at an earlier stage and that to the right indicates that it extended to a later

stage) [1]. The  $\theta$  is the infected days standardized to range from  $-5$  to  $5$ .

### **2.2.3. The QE Model**

The quadratic equation model (QE) was proposed for projecting the future CNCC [19] using Equation (6):

$$Y_i = ax_i^2 + bx_i + c, (6)$$

where  $Y_i$  denotes the CNCC at the  $i$ th day,  $x_i$  is the  $i-1$  infected days, and  $c$  represents the CNCC at the first day.

In the QE model, there are three points,  $P1 = (x1, y1)$ ,  $P2 = (x2, y2)$ , and  $P3 = (x3, y3)$ , on the trajectory CNCCs. As such,  $y1$  denotes the corresponding number of cases on day 1 (i.e.,  $x1 = 0$ ),  $y2$  corresponds to the CNCCs on the middle, and  $y3$  corresponds to the CNCCs on the present day. The model parameters, which are similar to the EXPO and IRT models, can be estimated by minimizing the model residual using the Microsoft add-in tool [2]; details are given in Additional file 1 (e.g., executing the procedural, SolverSolve UserFinish: = True, ShowRef: = "ShowTrial", using visual basic for applications (VBA)).

## **2.3. Scenarios in the Short and Long Terms during the COVID-19 Pandemic**

The three mathematical models mentioned above were compared in two scenarios based on the time-frame stages, including the early 20 days and the entire year in 2020. Whether different models yield disparate negative impact hit by COVID-19 in the two scenarios was

verified in this study.

## 2.4. Analysing Model Accuracy (MA) and Prediction Power (PP)

Both statistics of the  $R^2$  model and mean absolute percentage error (MAPE) were applied to evaluate the MA and the PP on the two time-frame scenarios (see the training and testing samples shown in Figure 1). We applied the model parameters calibrated in the training sample to predict the CNCC in the testing sample by observing the two measures of  $R^2$  and MAPE. The  $R^2$  and MAPE are defined in Equations (7)–(8):

$$R^2 = 1 - \frac{\text{model residual}}{\sum_{i=1}^n (O_i - \hat{O})^2} \quad (7)$$
$$\text{SUMXMY2}(\{E_i\}, \{O_i\}) = \sum_{i=1}^n (O_i - E_i)^2 \quad (8)$$

where  $O_i$  denotes the observed CNCC and  $\hat{O}$  is the mean CNCC in a given country/region.

The model residual is computed by Equation (8).  $E_i$  represents the expected CNCC.

$$\text{MAPE} = \frac{1}{n} \times \sum_{i=1}^n \left| \frac{O_i - E_i}{O_i} \right|, \quad (9)$$

where  $O_i$  is the observed CNCC and  $E_i$  is the predicted CNCC. The absolute value in Equation (8) is summed across all predicted points in days and divided by the numbers of fitted point  $n$ .

===Figure 1 inserted here===.

## 2.5. Introducing Angle Index

The forest plot [23] was used to examine the difference in  $R^2$  and MAPE. The first step was to compare the effects of  $R^2$  and MAPE in the three mathematical models at the early outbreak stage. The second step was to observe the difference in  $R^2$  and MAPE in 2020 based

on two best-fit models selected in the first step.

The angle index defined in Equation (9) was used to measure the negative impact hit by COVID-19:

$$\text{Angle index} = \theta = \text{Degrees} \left( \text{Atan} \left( \frac{\Delta \text{CNCC}_k}{\Delta \text{IP}_k} \right) \right), (10)$$

where both Degrees () and Atan () are derived from the functions in Microsoft Excel, and the IP denotes the inflection point [1] on the trajectory of  $\Delta \text{CNCC}$  (see the example in Introduction).

## 2.6. Angle Index Computed for Different Countries

The choropleth maps [24] were used to present the angle indexes for countries/regions at the early stage and in the entire year of 2020. The darker color in countries/regions represents more severe impact. When the region color is clicked, line plots used to predict the future CNCCs are generated through different mathematical models.

## 2.7. Statistical Tools and Data Analysis

The mean and standard deviation (SD) were extracted to compare the standardized mean difference (SMD) in the forest plot. A significant level of type I error was set at 0.05.

Visual representations of the forest plot and choropleth map display the comparison of the difference in MA, PP. The angle indexes were plotted online on Google Maps. The parameter estimation was executed in Microsoft Excel (Additional file 1). The study flowchart is shown in Figure 1.

# Results

## 3.1. Task 1: Model Comparisons at the Early Outbreak Stage

Comparisons were made using the illustrative examples of Guangdong in China and New York in the US. Results show that the EXPO model is superior compared to the IRT and quadratic equation (QE) models when examining the trajectories of CNCCs at the early stage. As shown in the top panel in Figure 2, in Guangdong, China, model  $R^2 = 1.0, 0.99, 0.96$  and MAPE = 0.02, 0.06, and 0.30 for the EXPO, IRT, and QE models, respectively. In comparison, in New York, USA, model  $R^2 = 1.0, 1.0, 0.97$  and MAPE = 0.01, 0.29, and 0.04 for the EXPO, IRT, and QE models, respectively.

===Figure inserted here===

Comparisons of  $R^2$  (in the earlier 20-day stage) and MAPE (for the following seven days) are made in Figures 3 and 4, respectively. After using the three models, results show that China has the best fit in terms of  $R^2 = 0.99$  and MAPE = 0.05 and 0.07 compared with its counterparts in different continents and in the US. Based on Figures 2–4, at the early outbreak stage, the EXPO and IRT models were selected for subsequent comparison in the next run of the long-term period in 2020 because of three reasons: (1) relatively higher  $R^2$  (i.e., Panels 1 and 3 in Figure 3), (2) identical  $R^2$  (i.e., the middle panel in Figure 3), and (3) greater consistency in the two models in terms of their MAPE values (i.e., the middle panel in Figure 4).

===Figures 3 and 4 inserted here===

### **3.2. Task 2: Comparison of Angle Indexes at the Early Outbreak Stage**

The angle indexes based on the early 20-day outbreak stage are presented in Figure 5. We can see that the higher angle indexes are in Hubei Province (including Wuhan) in China as well as in New York and New Jersey in the US. The countries severely hit by COVID-19 are marked with darker colors, including Iran and Turkey, among others. Notably, the angle indexes were computed by the  $\Delta CNCC = CNCC$  at IP days (i.e.,  $\Delta IP = IP$  based on Equation (9)). Readers are invited to scan the QR-code in Figure 5 to examine the ogive curves for countries/regions of interest when the color region is clicked.

===Figure 5 inserted here===

### **3.3. Task 3: Comparison of the EXPO and IRT Models for the Year 2020**

Upon modeling the CNCC data in the EXPO and IRT models to estimate their parameters, the results revealed that the IRT model has significantly higher  $R^2$  and MAPE values, as shown in Figure 6. The forest plots were drawn by computing the respective pair-statistics of mean and SD values in  $R^2$  and MAPE, respectively.

Only South America and the US currently have the same highest  $R^2$  ( $>0.90$ ) between the two models. In other continents and in China, the IRT model has a higher  $R^2$  and smaller

MAPE than the EXPO model; see higher  $R^2$  in the left column (which favors the IRT) and lower MAPE in the right column (which also favors the IRT) in Figure 6.

===Figure 6 inserted here===

### **3.4. Task 4: Comparison of Angle Indexes in the Long Run**

The angle indexes based on the 2020 data are shown in Figure 7. As can be seen, the most negatively impacted countries were India, the UK, and the US (specifically California).

Notably, the angle is computed by the  $\Delta\text{CNCC}$  ( $=\text{CNCC at IP} - \text{CNCC at IP-6}$ ) divided by the

LID ( $=6$ ) in Figure 7. As such, the meaning of disease outbreak is reflected by the

ImpactCOVID, given that a common base of 7-day incubation period is applied to compute

the angle index. Readers are also invited to scan the QR-code in Figure 7 to examine the

ogive curves for countries/regions of interest when the color region is clicked. For example,

the two ogive curves of Hubei Province (including Wuhan) in China are compared using the

EXPO and IRT models. Although the two curves look similar, the projection curve in the IRT

model (shown at the bottom of Figure 7) has a higher  $R^2$  and a smaller MAPE than the EXPO

model (0.99 vs. 0.98 and 0% vs. 0.2%, respectively).

===Figure 7 inserted here===

### **3.5. Online Dashboards Shown on Google Maps**

All of the QR codes in the figures are linked to the dashboards. Readers are recommended to examine the displayed dashboards on Google Maps.

# Discussion

## 4.1. Principal Findings

We observed that (1) the EXPO and IRT models are superior to the QE model at the early outbreak stage; (2) the IRT model has a higher  $R^2$  model and smaller MAPE than the EXPO model in 2020; (3) as can be expected, Hubei Province in China has the highest angle index at the early outbreak stage; and (4) India, Brazil, and Russia had the highest angle indexes (based on the 7-day incubation period) in 2020.

## 4.2. Contributions of the Study

Although a previous study [2] had applied the IPcase index to examine the effective control of COVID-19, the angle index can be exactly reflected by the ImpactCOVID, as demonstrated in this study.

Many researchers [10–19] have proposed the use of mathematical models to predict the number of COVID-19 cases, while others have investigated the IP days during the COVID-19 pandemic [25–29]. None of these studies, however, used the IP days to compare the ImpactCOVID, nor did they apply the angle index to inspect the ImpactCOVID in countries/regions.

The second contribution of this study has to do with the comparison of mathematical COVID-19 models, which are used to predict the CNCCs in the future. Thus far, few studies have compared the MA and PP between models, which might be due to the fact that some

authors are not familiar with the algorithms proposed by authors of other works. In this work, we compared three mathematical models [2,18,19] based on common conditions (e.g., the evolution of CNCC and the  $\Delta IP = 7$  across countries/regions).

The EXPO model [18] has been verified in several regions in China, including Wuhan in Hubei Province, Guangdong Province, and other parts of Mainland China at an early outbreak stage (from 27 January to 18 February 2020). In comparison, this study featured (1) two time-frame stages (i.e., the early 20-day outbreak stage and the entire year of 2020) and (2) all countries/regions around the world.

The QE model [19] has been used to demonstrate the projected cases in Colombia as well as deaths in Russia, India, and the rest of the world using the past 31-day data up to 29 May 2020. In that work, the constrained term was set at the middle point (i.e.,  $P(x_2, y_2)$ ) of the observations with exponential growth during the COVID-19 epidemic.

Given that using less constrained parameters makes the model a better fit for the data [29,30], one constrained term set at the middle point (i.e.,  $P(x_2, y_2)$ ) of the observations in the QE model [19] yields lower MA accordingly. In contrast, the unconstrained QE model in this study (i.e., using the Solver add-in tool in Microsoft Excel) can yield higher MA than the constrained one. This is evidenced by the fact that the QE model is inferior to the EXPO or the IRT model, or even the unconstrained QE model.

Another study [2] applied IRT [30,31] to construct an ogive curve and determine the IP

days used for predicting the projected cases by country/region based on the CNCC. However, the drawback of the IRT model is that it involves another compression coefficient (called “CR” in [2]) to adjust the estimation of expected CNIC at the early outbreak stage. This is the reason why the IRT model is slightly inferior to the EXPO model when used in assessing impact at the early outbreak stage.

### **4.3. Implications and Recommendations**

Numerous mathematical COVID-19 models [10–19] and IP determinations [2,8,9] have been proposed in the literature. However, none developed an index that can be used to measure the ImpactCOVID. In this study, we overcome this problem by proposing the use of the angle index, as shown in Equation (9).

Many online real- or near-real-time dashboards have been launched for tracking the worldwide spread of the COVID-19 outbreak [32–37]. However, most of these are similar to other traditional websites [38–42] and merely provide the same information as the WHO COVID-Dashboard [34]. A more accurate assessment of COVID-19 requires further mathematical analyses of data reported worldwide [38]. Furthermore, although dashboards (e.g., JHU [32], WHO [34], and others [33,34,36,37]) have provided interesting visualizations for reporting the current state of COVID-19, these presentations lack important information about the disease outbreak using mathematical models to predict the projection of CNCCs in the future, which could be useful in understanding the trends of COVID-19 [19].

One study [42] assessed 158 public Web-based COVID-19 dashboards and found that only a few dashboards employed predictive analytics by demonstrating various future scenarios. Thus, the imprecise predictive models and simulations early in the pandemic may have restricted their application. In the current study, we demonstrated the predictive approaches with a dashboard design that can benefit both policymakers and epidemiologists during the COVID-19 epidemic.

#### **4.4. Strengths of the Study**

First, the comparison of the ImpactCOVID using the angle index in countries/regions can be applied to future relevant studies and is not limited to those merely focusing on the COVID-19 pandemic.

Second, MP4 videos on how to model the CNCC and estimate the parameters for mathematical models have been provided to ordinary readers who are familiar with Microsoft Excel and hope to replicate the study in the future.

Third, using the Microsoft Solver add-in to estimate the model parameters is a common approach that can be easily applied by researchers [2,4,43–45]. Data and model building videos are provided in Additional file 1. The approach of searching IP days that can be used for computing the angle index has been demonstrated in [2].

Fourth, the choropleth and forest plot diagrams used in this study are able to provide comprehensive insights into the evolution of the COVID-19 pandemic in various

countries/regions, which in turn can be used by policymakers and decision-makers.

Furthermore, an MS Excel module for drawing the forest plot is provided. Readers are recommended to see the abstract video along with the Excel module presented in Additional file 1.

#### **4.5. Limitations and Future Studies**

Our study has several limitations that should be mentioned. First, only three mathematical models were compared to assess MA and PP. Future studies are required to study more COVID-19 models for better comparison.

Second, only short- and long-term time periods during the COVID-19 pandemic were compared using the models. Determining whether differences in MA and PP exist in the medium-term (or mid-term) epidemic is worthy of further studies in the future.

Third, the case number is changeable and may vary day by day, particularly in countries undergoing second or third waves (peaks) in the ongoing pandemic. Thus, model parameters and angle indexes would also vary as time passes.

Fourth, the Microsoft Solver add-in is not a unique approach in estimating model parameters. Thus, many other methods and mathematical techniques should be used in making estimations and comparisons in the future.

Fifth, visual dashboards on Google Maps are not free of charge, and a paid project key for using the Google cloud platform is required. Thus, one limitation in using the dashboard is

that it cannot be easily replicated by other authors or programmers for use in a short period of time.

Finally, although the IRT evidently has better MA and PP in the long run, other user-friendly mathematical models are also available for readers to understand the properties of exponential growth and the quadratic equation in nature. These can be used in building better COVID-19 models for further comparisons in the future.

## **Conclusions**

The three proposed models were compared in terms of their MA and PP in two time-frame scenarios, namely, the early outbreak stage and across the entire year of 2020. We found that the IRT model is superior to the QE and EXPO models in the long term, whereas the EXPO model is better at the early stage. This is because only the ogive curves that occurred in the IRT model can generate the IP, which can then be used to compute the angle index. Both models are recommended so that readers can accurately project the CNCCs in other outbreak scenarios in the future and not just those of the COVID-19 pandemic.

### **List of abbreviations:**

CNCC: cumulative number of confirmed cases

EXPO: exponential growth

ImpactCOVID: impacts of the COVID-19 outbreak

IRT: item response theory

LID: the length of infected days effectively under control

MA: model accuracy

MAPE: mean absolute percentage error

PP:prediction power

QE:quadratic equation

## **Declarations**

### **Ethics approval and consent to participate**

Not applicable.

All data were downloaded from the website database at Github

### **Consent to publish**

Not applicable.

### **Availability of data and materials**

All data used in this study are available in Additional Files.

### **Competing interests**

The authors declare that they have no competing interests.

### **Funding**

There are no sources of funding to be declared.

### **Authors' contributions**

T.-W.C. developed the study. D.-H.Y., T.-Y.Y., and W.C. analyzed the data. K.-T.T. monitored the process of this study and helped in responding to the reviewers' advice and comments. T.-W.C. drafted the manuscript, and all authors provided critical revisions for important intellectual content. The study was supervised by K.-T.T. All authors have read and agreed to the published version of the manuscript.

### **Acknowledgments**

We thank AJE (American Journal Experts at <https://www.aje.com/>) for the English language review of this manuscript. All authors declare no conflicts of interest.

# Additional Files

## Additional file 1:

Data and MP4 video of model building at

[https://osf.io/4pmn7/?view\\_only=5afba393509746bd8a332b2c65839034](https://osf.io/4pmn7/?view_only=5afba393509746bd8a332b2c65839034) (accessed on 19

April 2021)

## References

1. Wiki. Disease Outbreak. Available online: [https://en.wikipedia.org/wiki/Disease\\_outbreak](https://en.wikipedia.org/wiki/Disease_outbreak) (accessed on 10 March 2021).
2. Wang, L.-Y.; Chien, T.-W.; Chou, W. Using the IPcase Index with Inflection Points and the Corresponding Case Numbers to Identify the Impact Hit by COVID-19 in China: An Observation Study. *Int. J. Environ. Res. Public Health* 2021, 18, 1994, doi:10.3390/ijerph18041994.
3. Chang, C.S.; Yeh, Y.T.; Chien, T.W.; Lin, J.J.; Cheng, B.W.; Kuo, S.C. The computation of case fatality rate for novel coronavirus (COVID-19) based on Bayes theorem: An observational study. *Medicine* 2020, 99, e19925.
4. Fisman, D.; Rivers, C.; Lofgren, E.; Majumder, M.S. Estimation of MERS-Coronavirus Reproductive Number and Case Fatality Rate for the Spring 2014 Saudi Arabia Outbreak: Insights from Publicly Available Data. *PLoS Curr.* 2014, 6, 6, doi:10.1371/currents.outbreaks.98d2f8f3382d84f390736cd5f5fe133c.

5. Yie, K.-Y.; Chien, T.-W.; Yeh, Y.-T.; Chou, W.; Su, S.-B. Using Social Network Analysis to Identify Spatiotemporal Spread Patterns of COVID-19 around the World: Online Dashboard Development. *Int. J. Environ. Res. Public Health* 2021, 18, 2461, doi:10.3390/ijerph18052461.
6. Hirsch, J.E. An index to quantify an individual's scientific research output. *Proc. Natl. Acad. Sci. USA* 2005, 102, 16569–16572, doi:10.1073/pnas.0507655102.
7. Fenner, T.; Harris, M.; Levene, M.; Bar-Ilan, J. A novel bibliometric index with a simple geometric interpretation. *PLoS ONE* 2018, 13, e0200098, doi:10.1371/journal.pone.0200098.
8. Chien, T.W. Trend of COVID-19 Using 7-day Mean Number of Confirmed Cases. Available online: <http://www.healthup.org.tw/html100/searchpubmed.asp> (accessed on 10 March 2021).
9. Fan, R.G.; Wang, Y.B.; Luo, M.; Zhang, Y.Q.; Zhu, C.P. SEIR-Based COVID-19 Transmission Model, and Inflection Point Prediction Analysis. *Dianzi Keji Daxue Xuebao J. Univ. Electron. Sci. Technol. China* 2020, 49, 369–374, doi:10.12178/1001-0548.9\_2020029.
10. Perc, M.; Miksić, N.G.; Slavinec, M.; Stožer, A. Forecasting COVID-19. *Front. Phys.* 2020, 8, 127, doi:10.3389/fphy.2020.00127.
11. Fang, Y.; Nie, Y.; Penny, M. Transmission dynamics of the COVID-19 outbreak and

- effectiveness of government interventions: A data-driven analysis. *J. Med. Virol.* 2020, 92, 645–659, doi:10.1002/jmv.25750.
12. Wu, J.T.; Leung, K.; Leung, G.M. Nowcasting and forecasting the potential domestic and international spread of the 2019-nCoV outbreak originating in Wuhan, China: A modelling study. *Lancet* 2020, 395, 689–697, doi:10.1016/s0140-6736(20)30260-9.
13. Anastassopoulou, C.; Russo, L.; Tsakris, A.; Siettos, C. Data-based analysis, modelling and forecasting of the COVID-19 out-break. *PLoS ONE* 2020, 15, e0230405, doi:10.1371/journal.pone.0230405.
14. Zhao, S.; Chen, H. Modeling the epidemic dynamics and control of COVID-19 outbreak in China. *Quant. Biol.* 2020, 8, 11–19, doi:10.1007/s40484-020-0199-0.
15. Rong, X.; Yang, L.; Chu, H.; Fan, M. Effect of delay in diagnosis on transmission of COVID-19. *Math. Biosci. Eng.* 2020, 17, 2725–2740, doi:10.3934/mbe.2020149.
16. Mandal, M.; Jana, S.; Nandi, S.K.; Khatua, A.; Adak, S.; Kar, T. A model based study on the dynamics of COVID-19: Prediction and control. *Chaos Solitons Fractals* 2020, 136, 109889, doi:10.1016/j.chaos.2020.109889.
17. Huang, J.; Qi, G. Effects of control measures on the dynamics of COVID-19 and double-peak behavior in Spain. *Nonlinear Dyn.* 2020, 101, 1889–1899, doi:10.1007/s11071-020-05901-2.
18. Shang, C.; Yang, Y.; Chen, G.-Y.; Shang, X.-D. A simple transmission dynamics model for

- predicting the evolution of COVID-19 under control measures in China. *Epidemiol. Infect.* 2021, 149, 1–10, doi:10.1017/s0950268821000339.
19. Florez, H.; Singh, S. Online dashboard and data analysis approach for assessing COVID-19 case and death data. *F1000 Res.* 2020, 9, 570, doi:10.12688/f1000research.24164.1.
20. Google Team. 2019 Novel Coronavirus (nCoV) Data Repository. Available online: <https://github.com/CSSEGISandData/2019-nCoV> (accessed on 19 October 2020).
21. Shang, X.-D.; Tong, P.; Xia, K.-Q. Scaling of the Local Convective Heat Flux in Turbulent Rayleigh-Bénard Convection. *Phys. Rev. Lett.* 2008, 100, 244503, doi:10.1103/physrevlett.100.244503.
22. Shang, X.-D.; Liang, C.-R.; Chen, G.-Y. Spatial distribution of turbulent mixing in the upper ocean of the South China Sea. *Ocean Sci.* 2017, 13, 503–519, doi:10.5194/os-13-503-2017.
23. Yan, Y.-H.; Chien, T.-W. The use of forest plot to identify article similarity and differences in characteristics between journals using medical subject headings terms. *Medicine* 2021, 100, e24610, doi:10.1097/md.00000000000024610.
24. Chien, T.-W.; Wang, H.-Y.; Hsu, C.-F.; Kuo, S.-C. Choropleth map legend design for visualizing the most influential areas in article citation disparities. *Medicine* 2019, 98, e17527, doi:10.1097/md.00000000000017527.

25. Buan, Q.; Wu, J.; Wu, G.; Wang, Y.G. Predication of Inflection Point and Outbreak Size of COVID-19 in New Epicentres. *Non-linear Dyn.* 2020, 101, 1561–1581.
26. Chatham, W.W. Treating Covid-19 at the Inflection Point. *J. Rheumatol.* 2020, 47, 1–10.
27. Gu, C.; Zhu, J.; Sun, Y.; Zhou, K.; Gu, J. The inflection point about COVID-19 may have passed. *Sci. Bull.* 2020, 65, 865–867, doi:10.1016/j.scib.2020.02.025.
28. Jeong, G.H.; Lee, H.J.; Lee, J.; Lee, J.Y.; Lee, K.H.; Han, Y.J.; Yoon, S.; Ryu, S.; Kim, D.K.; Park, M.B.; et al. Effective Control of COVID-19 in South Korea: Cross-Sectional Study of Epidemiological Data. *J. Med. Internet Res.* 2020, 22, e22103, doi:10.2196/22103.
29. Gallacher, D.; Kimani, P.; Stallard, N. Extrapolating Parametric Survival Models in Health Technology Assessment: A Si-mu-lation Study. *Med. Decis Making.* 2021, 41, 37–50.
30. Van Rijn, P.W.; Sinharay, S.; Haberman, S.J.; Johnson, M.S. Assessment of fit of item response theory models used in large-scale educational survey assessments. *Large-Scale Assess. Educ.* 2016, 4, 1, doi:10.1186/s40536-016-0025-3.
31. Lord, F.M. *Applications of Item Response Theory to Practical Testing Problems*; Lawrence Erlbaum Associates: Hillsdale, NJ, USA, 1980.
32. NBSP; Johns Hopkins University Coronavirus Resource Center. COVID-19 Dashboard by the Center for Systems Science and Engineering (CSSE) at Johns Hopkins University (JHU). Available online: <https://coronavirus.jhu.edu/map.html> (accessed on 29 October 2020).

33. Leszkiewicz, A. Dashboard Online for COVID-19 in Near Real Time. Available online:  
<https://avatorl.org/covid-19/> (accessed on 20 February 2021).
34. World Health Organization. WHO Coronavirus Disease (COVID-19) Dashboard. 2020.  
Available online: <https://covid19.who.int/> (accessed on 3 March 2021).
35. HealthMap. Novel Coronavirus 2019-nCoV (Interactive Map). Available online:  
<https://healthmap.org/wuhan/> (accessed on 20 February 2021).
36. Schiffmann, A. A Creator of One COVID-19 Dashboard. Available online:  
<https://ncov2019.live/data> (accessed on 20 February 2021).
37. Dong E, Du H, Gardner L. An interactive web-based dashboard to track COVID-19 in real time. *Lancet Infect Dis.* 2020 May;20(5):533-534. doi: 10.1016/S1473-3099(20)30120-1.
38. WHO. Novel Coronavirus (2019-nCoV) Outbreak. Available online:  
<https://www.who.int/emergencies/diseases/novel-coronavirus-2019/situation-reports>  
(accessed on 10 August 2020).
39. Centers for Disease Control and Prevention. Available online: <http://www.cdc.gov/>  
(accessed on 6 February 2013).
40. European Centre for Disease Prevention and Control (ECDC). Novel Coronavirus.  
Available online: <https://www.ecdc.europa.eu/en/home> (accessed on 20 February 2021).
41. DXY. Novel Coronavirus (2019-nCoV). Available online:  
<https://ncov.dxy.cn/ncovh5/view/pneumonia> (accessed on 20 February 2021).

42. Ivanković, D.; Barbazza, E.; Bos, V.; Fernandes, Óscar, B.; Gilmore, K.J.; Jansen, T.; Kara, P.; Larrain, N.; Lu, S.; Meza-Torres, B.; et al. Features Constituting Actionable COVID-19 Dashboards: Descriptive Assessment and Expert Appraisal of 158 Public Web-Based COVID-19 Dashboards. *J. Med. Internet Res.* 2021, 23, e25682, doi:10.2196/25682.
43. Yan, Y.-H.; Chien, T.-W.; Yeh, Y.-T.; Chou, W.; Hsing, S.-C. An App for Classifying Personal Mental Illness at Workplace Using Fit Statistics and Convolutional Neural Networks: Survey-Based Quantitative Study. *JMIR mHealth uHealth* 2020, 8, e17857, doi:10.2196/17857.
44. Ma, S.-C.; Chou, W.; Chien, T.-W.; Chow, J.C.; Yeh, Y.-T.; Chou, P.-H.; Lee, H.-F. An App for Detecting Bullying of Nurses Using Convolutional Neural Networks and Web-Based Computerized Adaptive Testing: Development and Usability Study. *JMIR mHealth uHealth* 2020, 8, e16747, doi:10.2196/16747.
45. Lee, Y.-L.; Chou, W.; Chien, T.-W.; Chou, P.-H.; Yeh, Y.-T.; Lee, H.-F.; Jen, T.-H. An App Developed for Detecting Nurse Burnouts Using the Convolutional Neural Networks in Microsoft Excel: Population-Based Questionnaire Study. *JMIR Med. Inform.* 2020, 8, e16528, doi:10.2196/16528.

## Figures legends

Figure 1 Study flowchart

Figure 2. Comparison of accuracy among the three proposed models.

Figure 3. Comparison of  $R^2$  values across continents, China, and the US based on the three models.

Figure 4. Comparison of MAPE values for the next week across continents, China, and the

US based on the three models.

Figure 5. The negatively impacted countries by COVID-19 identified using the angle index.

Figure 6. Comparison of the R2 square and MAPE values between the EXPO and IRT models using forest plots.

Figure 7. Top three countries are experiencing the most severe impact of COVID-19 based on angle index (top) and the comparison of modeling effects between the EXPO and IRT models.

# Figures

## Ourbreak Period **A. Model selection**

Short term:  
First 23 days

Comparison of 3 mathematical models:

1. Expo
2. IRT
3. QE

Selection of the best one with the higher  $R^2$  in prediction & the lower PAPE in next 7 days

Long term:  
Year 2020

Between two mathematical models

- EXPO : The exponential growth model
- IRT : Item response theory model
- QE : The quadratic equation model

Start

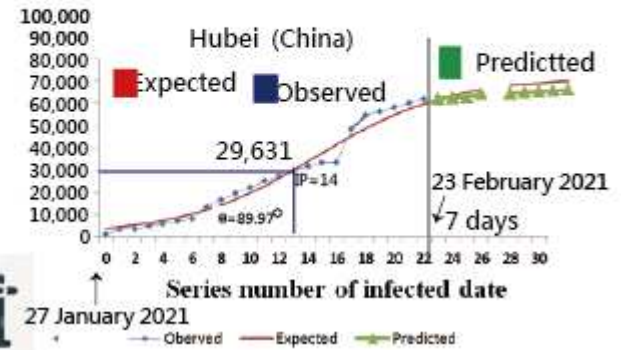
COVID-19 Data



End

## **B. Impact denoted by angle index**

Infected Case



Scenarios: 1. early stage 2. entire year  
Sample: (Training + Testing) (Training + Testing)

Impact hit by COVID-19 using the angle(=  $\theta$ )

= DEGREES (ATAN (Case/IP days))  
in MS Excel

MS : Microsoft

IP : inflection point

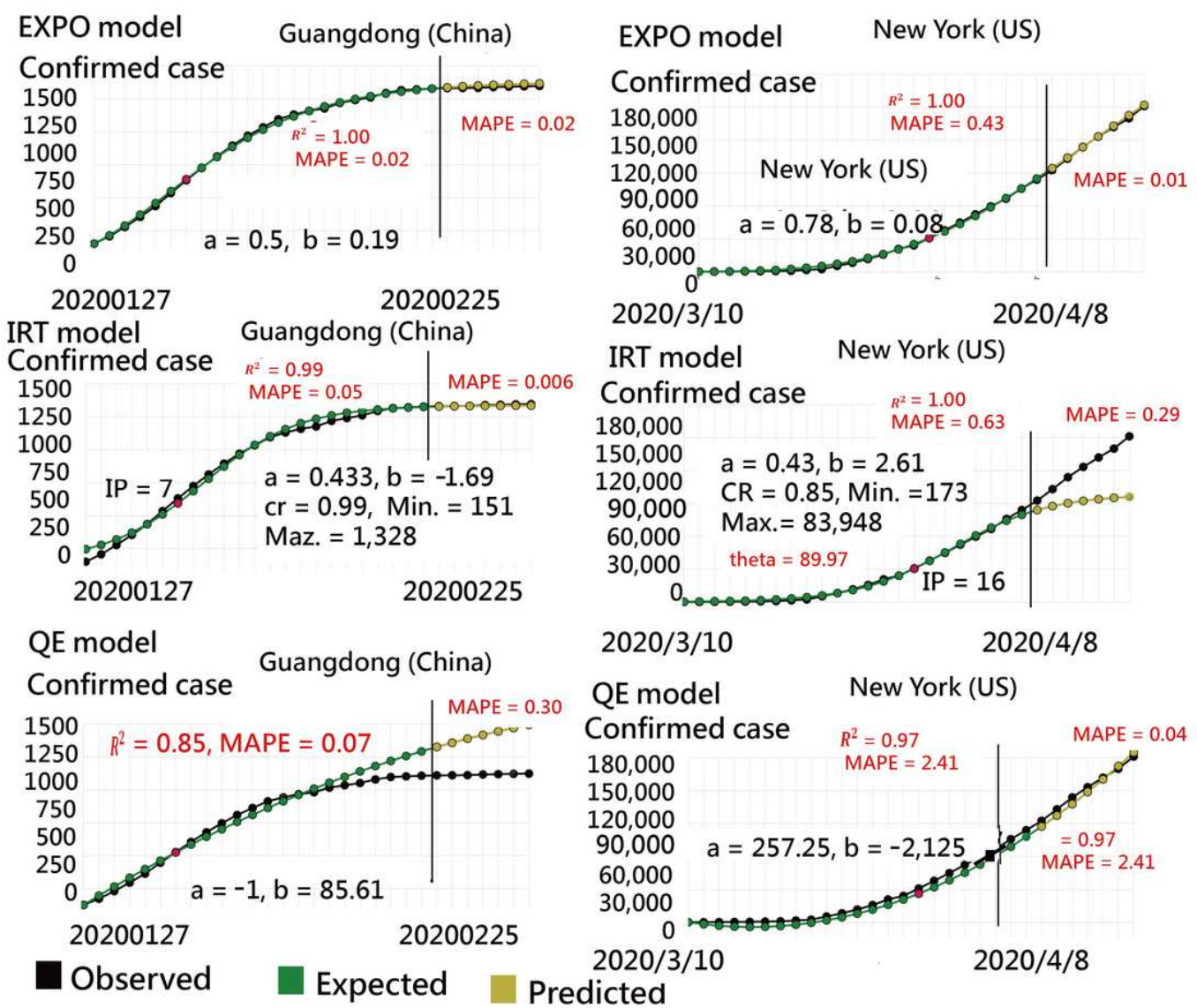
DEGREES : Function in MS Excel

ATAN : Function in MS Excel

$R^2$  : Explained by variance

Figure 1

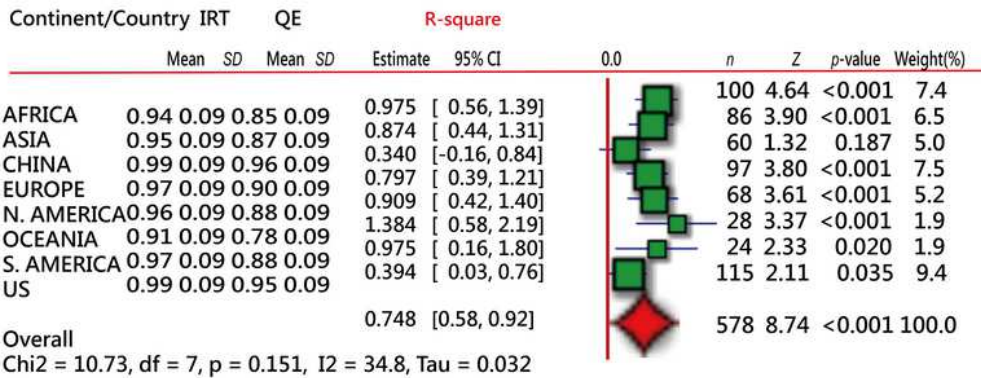
Study flowchart



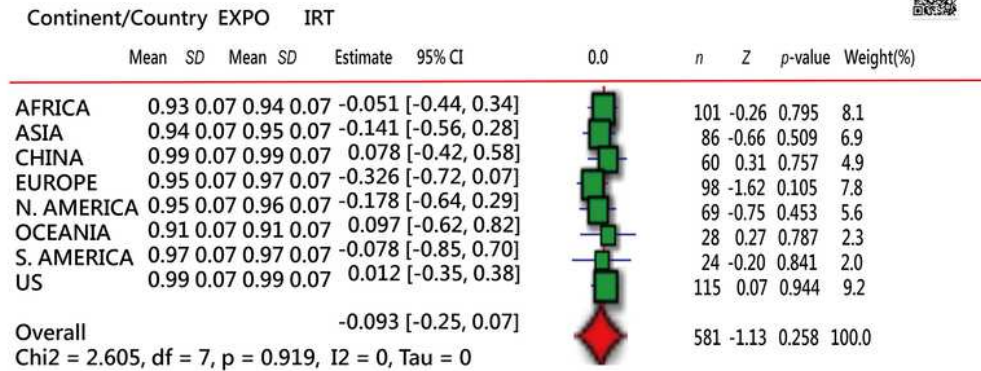
EXPO : The exponential growth model  
 IRT : Item response theory model  
 QE : The quadratic equation model'  
 Max. : Maximum in accumulative case number  
 theta : Standardized logit value in days

a : Slope parameter in IRT model  
 b : Location parameter in IRT model  
 CR : Compressed coefficient  
 Min. : Minimum in accumulative case number

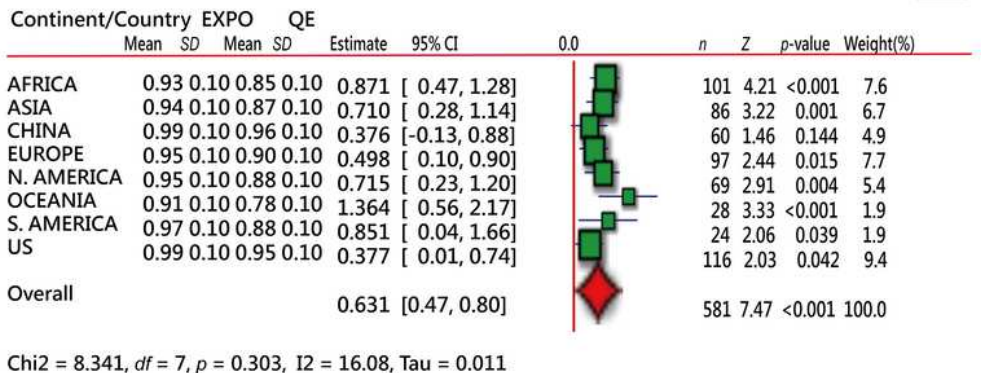
**Figure 2**  
 Comparison of accuracy among the three proposed models.



Favors QE    Favors IRT



No difference in R<sup>2</sup>



EXPO : The exponential growth model

IRT : Item response theory model

QE : The quadratic equation model

Chi2 : Chi-square

df : degree of freedom

I2 : I-square in Meta-Analysis

Tau : Tau square of variance in Meta-Analysis

CI : Confidence Interval

Favors QE    Favors EXPO

R<sup>2</sup>: Explained by variance

Variable effect

Overall fixed effect

Mean : Average value

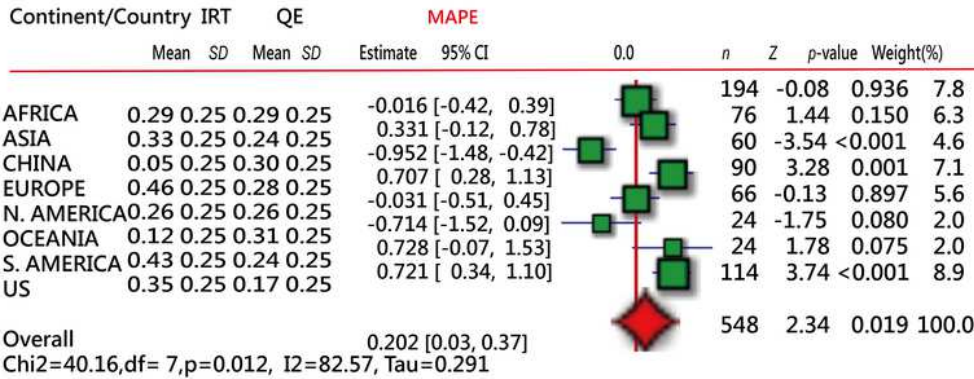
SD : Standard Deviation

Z : Z-score

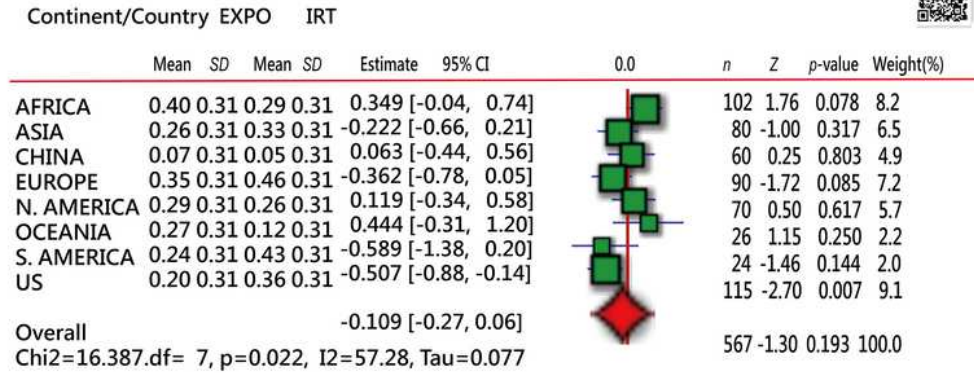


Figure 3

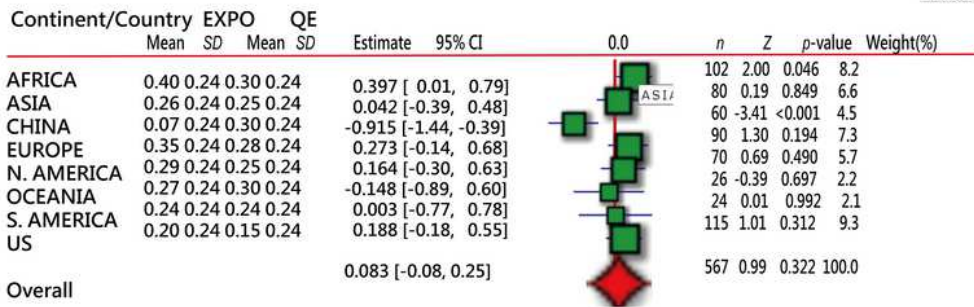
Comparison of R<sup>2</sup> values across continents, China, and the US based on the three models.



Favors IRT    Favors QE



Favors EXPO    Favors IRT



(MAPE in next 1 week)  
Chi2=18.055, df= 8, p=0.012, I2=61.23, Tau=0.091

EXPO : The exponential growth model  
IRT : Item response theory model  
QE : The quadratic equation model  
Chi2 : Chi-square  
df : degree of freedom  
I2 : I-square in Meta-Analysis  
Tau : Tau square of variance in Meta-Analysis  
CI : Confidence Interval

Favors EXPO    Favors QE

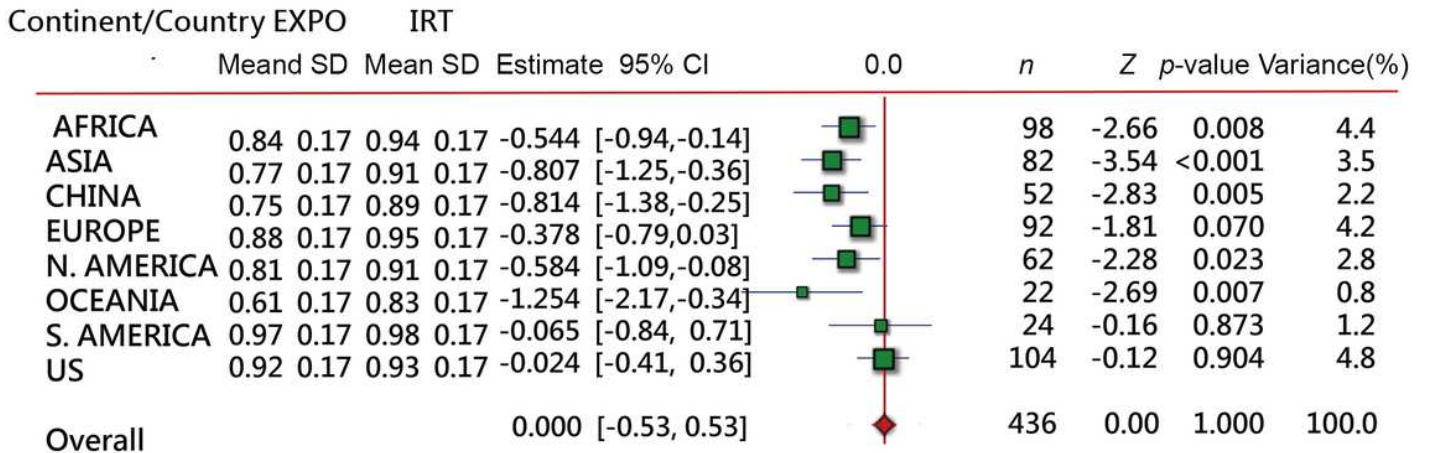
R<sup>2</sup>: Explained by variance

Variable effect    Overall fixed effect  
Mean : Average value  
SD : Standard Deviation  
Z : Z-score

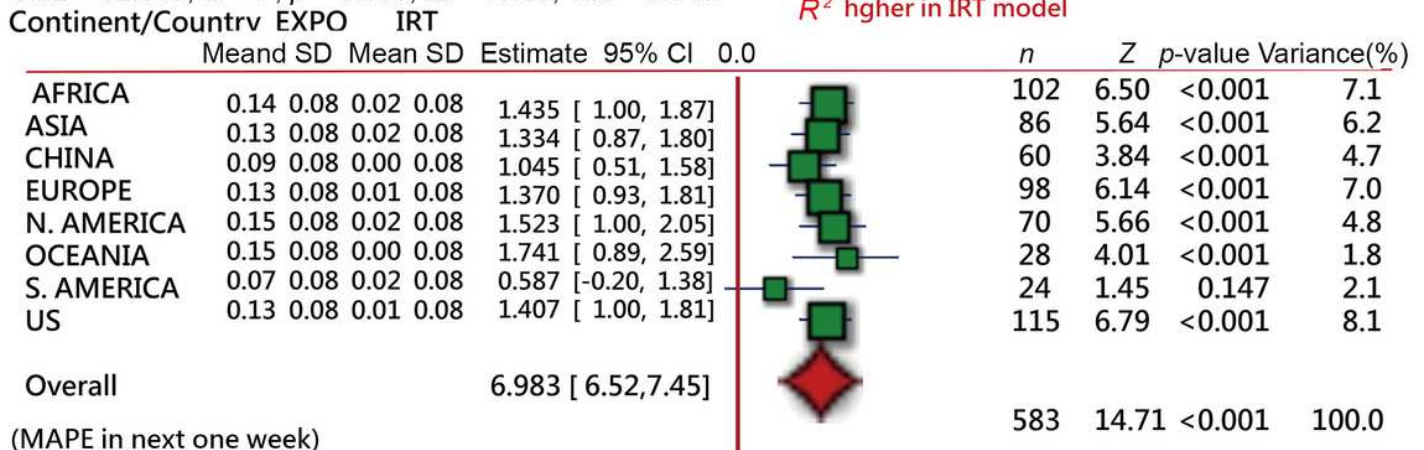


Figure 4

Comparison of MAPE values for the next week across continents, China, and the US based on the three models.



Chi2 = 32.947, df = 7, p = 0.199, I2 = 18.05, Tau = 0.016



(MAPE in next one week)

Chi2 = 6.29, df=7, p = 0.506, I2 = 0, Tau = 0

MAPE (prediction) in next 1 week lower in IRT model

EXPO : The exponential growth model

IRT : Item response theory model

QE : The quadratic equation model

Chi2 : Chi-square

df : degree of freedom

I2 : I-square in Meta-Analysis

Tau : Tau square of variance in Meta-Analysis

S, AMERICA : South America

MAPE : mean absolute percentage error

CI : Confidence Interval

■ Variable effect

◆ Overall fixed effect

R<sup>2</sup>: Explained by variance

Mean : Average value

SD : Standard Deviation

N AMERICA : North America

Z : Z-score



Figure 5

The negatively impacted countries by COVID-19 identified using the angle index.

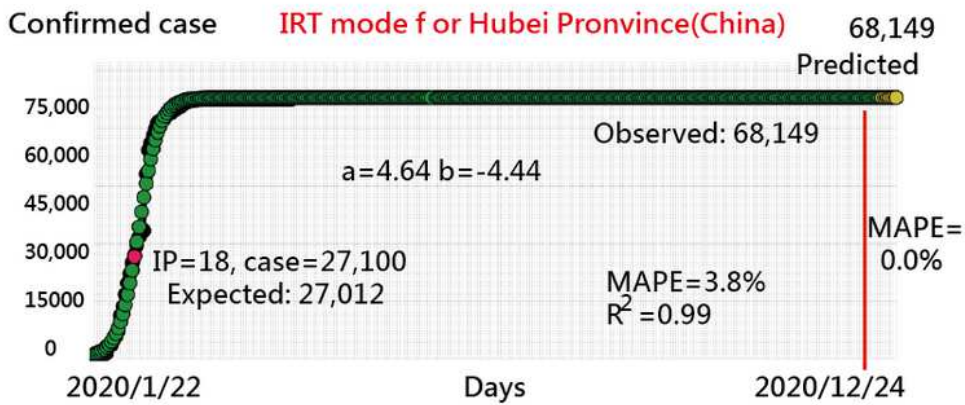
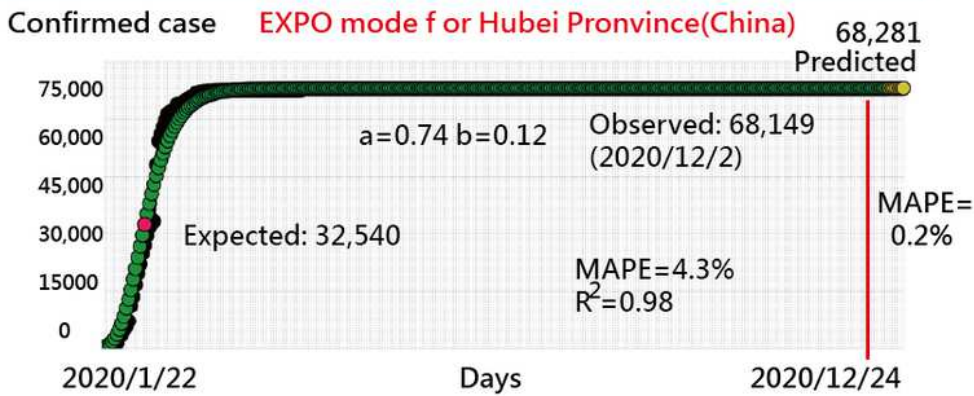
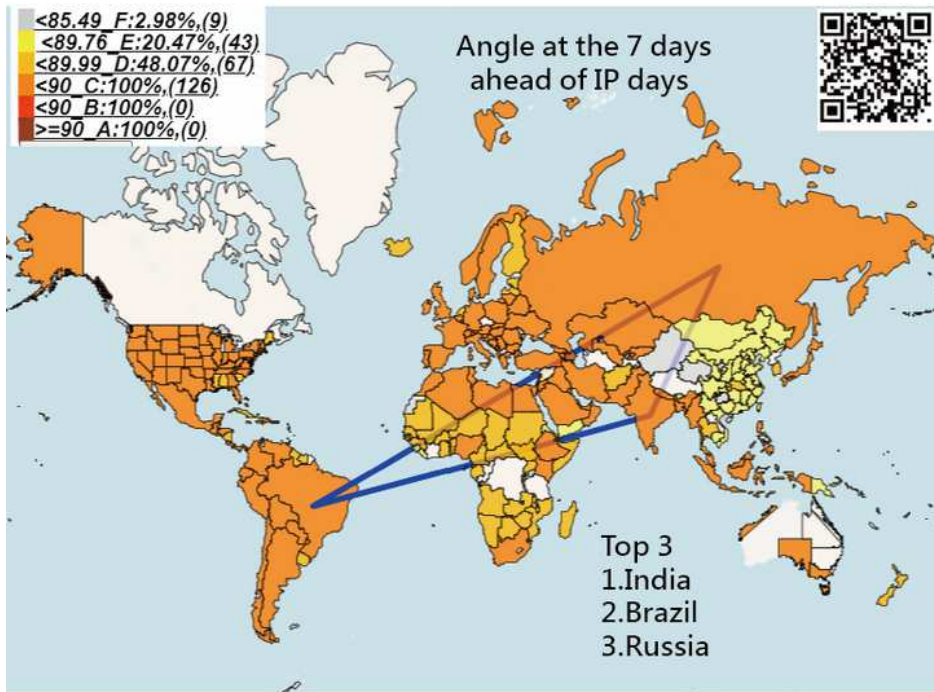


Figure 6

Comparison of the R2 square and MAPE values between the EXPO and IRT models using forest plots.

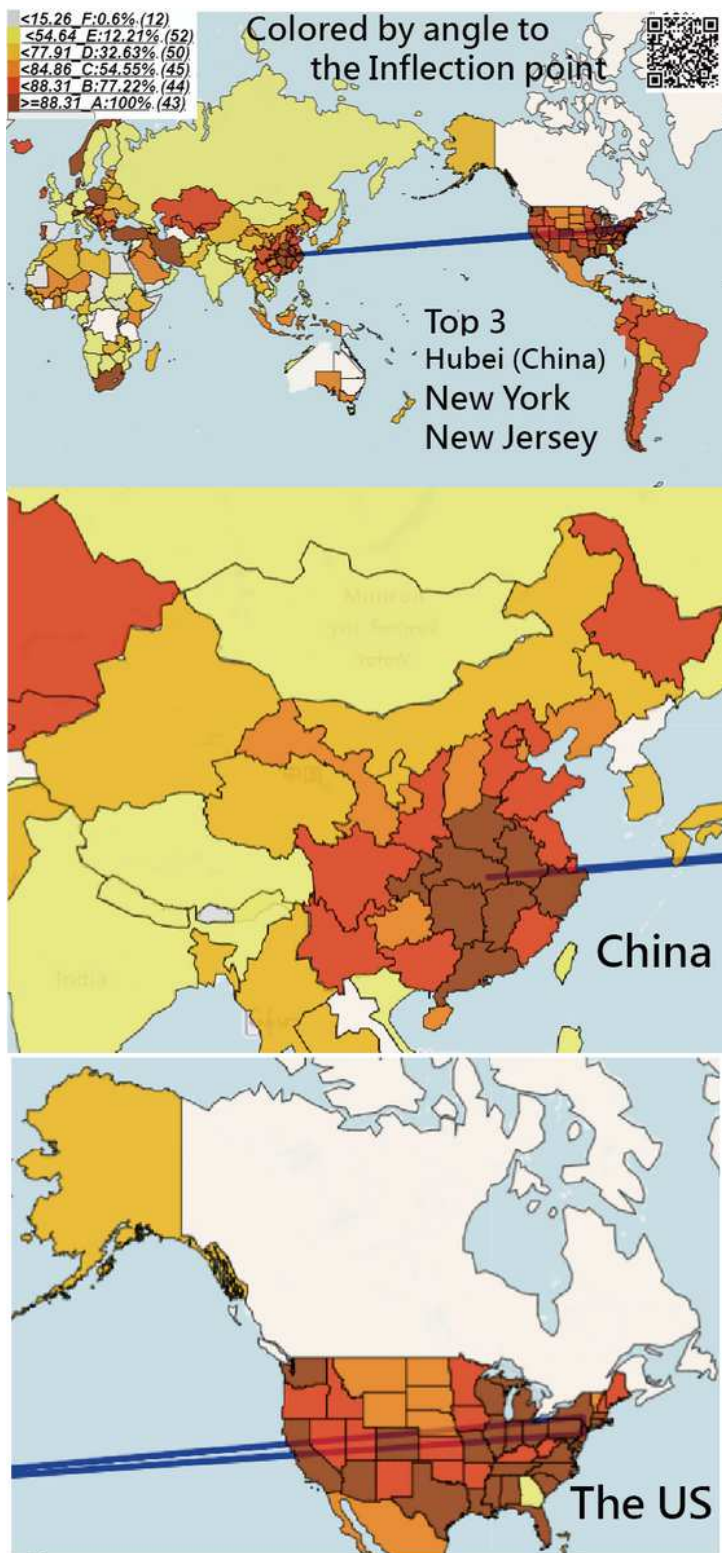


Figure 7

Top three countries are experiencing the most severe impact of COVID-19 based on angle index (top) and the comparison of modeling effects between the EXPO and IRT models.

## Supplementary Files

This is a list of supplementary files associated with this preprint. Click to download.

- [additionfile1.txt](#)